PCCP

COMMUNICATION

View Article Online
View Journal | View Issue

Cite this: *Phys. Chem. Chem. Phys.*, 2014, **16**, 19832

Received 17th July 2014,
Accepted 29th July 2014

DOI: 10.1039/c4cp03168g

www.rsc.org/pccp

Mechanistic insights into the reduction of graphene oxide addressing its surfaces†

Siegfried Eigler

Both sides of a graphene oxide (ai-GO) layer are decorated with functional groups. For the first time it is demonstrated that an effective reduction of ai-GO to graphene can be performed, even if the reducing agent can access only one side of ai-GO. A general reduction mechanism is proposed.

Graphene oxide (GO) and graphene are nanomaterials that have attracted interdisciplinary attention in the field of physics, as well as chemistry and medicine.[1–3] GO can be prepared in large quantities, is water-processible and of technological interest.[4] It possesses a carbon framework arranged in a honeycomb lattice, which is chemically functionalized with oxo-functional groups on both sides of the carbon lattice.[5] Treating GO with reducing agents leads to the formation of single layers of graphene (G_1, index indicates the number of layers) with a variable density of defects.[6–8] The mobility of charge carriers depends on the density of defects and therefore, mobility values range between 0.1 and 1000 $cm^2\ V^{-1}\ s^{-1}$.[9] GO is often deposited on substrates and reduced to G_1.[10] Consequently, the reducing agent can access GO from the upper side, because diffusion of the reducing agent between the substrate and the GO layers appears to be unfavoured. The improvement of the reduction process is a crucial question of synthetic and technological interest.[4,11,12] It can be anticipated that a reduction process could be more efficient if both sides of GO would be unhindered accessible.

GO is commonly prepared from natural graphite in sulphuric acid using potassium permanganate as an oxidant to oxo-functionalize graphite.[13–15] It turned out that the reaction and work-up procedure can be controlled, avoiding over-oxidation that would lead to permanent defects due to the evolution of CO_2 and thus, the loss of lattice carbon atoms.[9,16] The density of defects of GO with an almost intact carbon framework (ai-GO) can be analysed after reduction by Raman spectroscopy of G_1. In mean the density of defects can be determined to be about 0.3% in average, in contrast to about 0.01% for the best quality of flakes.[8,9,17–20] Ai-GO is an attractive starting material for derivatisation,[21] excluding manifold reactions at edges of defects.[5] Recently, ai-GO was used to determine the thermal stability of the carbon framework,[22] and a mixture of hydriodic acid and trifluoroacetic acid (HI–TFA) and ascorbic acid (AS) were identified as highly efficient reducing agents for ai-GO.[8,23,24]

Since Raman spectroscopy on G_1 is the most reliable method to determine its quality, ai-GO is commonly placed on a substrate and subsequently chemically reduced to determine the density of defects.[18] After placing ai-GO on a substrate the faces of ai-GO can be distinguished. It can be assumed that the diffusion of liquid or gaseous reducing agents between the substrate (Si/300 nm SiO_2) and ai-GO is hampered due to strong hydrogen bonding. Thus, only the upper side of ai-GO is easily accessible. Although, reduction in solution would give access to both sides, the aggregation to G_n (graphite) is inevitable in solution and a reliable Raman spectroscopic analysis of few-layer graphene or even graphite is hampered because of peak broadening.[18]

The quality of G_1 is of crucial importance for the electrical performance and thus, it is a fundamental question whether the quality of G_1 can be further increased if a reducing agent can access both sides of ai-GO unhindered.

Here, it is demonstrated that the reduction of ai-GO from one side is sufficient to generate G_1 of high quality (Fig. 1A). An aqueous solution of a reducing agent is used as a subphase to prepare films of floating graphene *via* the Langmuir–Blodgett technique. These graphene flakes are formed on the reductive subphase. After transferring this graphene on a substrate, vapours of HI–TFA are used for reduction, with access from the upper side. The density of defects is determined after each step by statistical Raman microscopy (SRM). By comparing the gathered results with experimental reference data it is confirmed that the reduction of ai-GO performed on a substrate from the upper

Department of Chemistry and Pharmacy and Institute of Advanced Materials and Processes (ZMP), Friedrich-Alexander-Universität Erlangen-Nürnberg (FAU), Dr.-Mack Str. 81, 90762 Fürth, Germany. E-mail: siegfried.eigler@fau.de; Fax: +49 911 6507865015; Tel: +49 911 6507865005

† Electronic supplementary information (ESI) available: General methods, preparation procedures, AFM and optical images, SRM results, and Raman spectra of ai-GO. See DOI: 10.1039/c4cp03168g

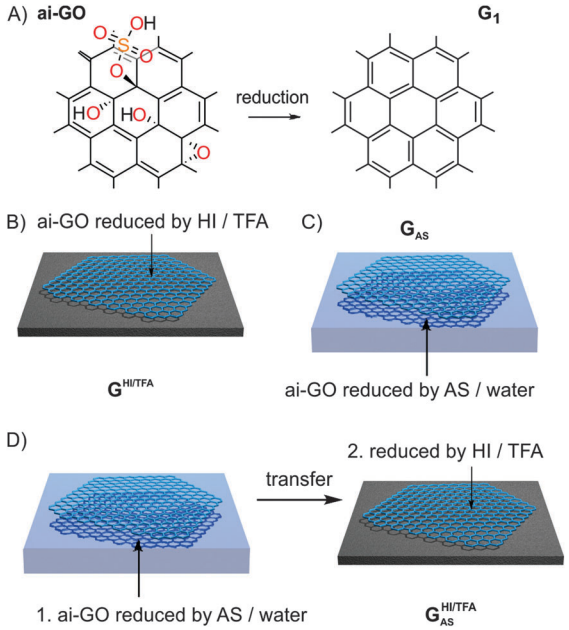

Fig. 1 (A) Scheme of the reduction of ai-GO to graphene (G_1); ai-GO reduced (B) on a substrate by vapours of HI–TFA ($G^{HI/TFA}$) (C) by AS from the reductive subphase (G_{AS}) and (D) combination of both reduction methods ($G_{AS}^{HI/TFA}$).

side is sufficient and effective. Thus, a simple mechanism for the reduction of ai-GO is proposed that involves successive protonation and electron transfer steps.

Ai-GO was synthesized according to the recently published procedure (SI) by oxidizing graphite in sulphuric acid with potassium permanganate at 5–10 °C and subsequent continuous dilution of the reaction mixture with water, keeping the temperature below 10 °C. Diluted H_2O_2 was used to dissolve manganese salts, and graphite oxide was purified by repeated centrifugation and redispersion steps in water. A minor fraction of graphite oxide already delaminates to single layers in water, however, ai-GO is mainly yielded after sonication. In previous publications ai-GO was characterised in detail.[9,18,25,26] Ai-GO bears hydroxyl groups, epoxy groups and organosulfate groups on both sides of the basal plane as illustrated in Fig. 1A.

Flakes of ai-GO were deposited on a Si/300 nm SiO_2 substrate as a film by the Langmuir–Blodgett (LB) technique (Fig. 2A). Another LB-film of ai-GO was prepared by floating flakes of ai-GO onto a reductive subphase of an aqueous solution of AS (1 mg ml^{-1}) or HI (1%, SI). After about 10 min, the LB-film becomes visible due to the formation of graphene and few-layer graphene (Fig. 2A and Fig. S2, ESI†). The LB-film was transferred after 90 min onto a Si/300 nm SiO_2 substrate. Another reduced ai-GO film was kept on the reductive subphase for 4 days and was analyzed directly while floating on the reductive subphase by SRM (Fig. S3, ESI†). It is even possible to visualize individual flakes floating on the reductive subphase by optical microscopy (Fig. 2B).

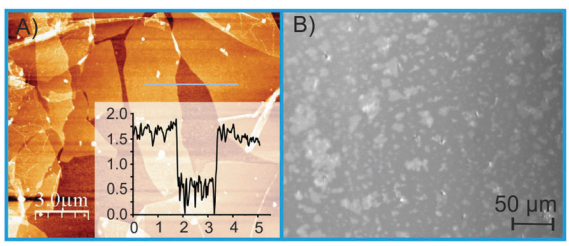

Fig. 2 (A) AFM image of ai-GO and height profile (in nm) along the grey line (in µm). (B) Optical microscope image of flakes of graphene floating on the reductive subphase.

As demonstrated before, HI–TFA or AS are highly effective reducing agents for ai-GO.[8] For SRM an area of 150 × 150 µm^2 of a film of flakes was probed and the intensities and full-widths at half-maximum (Γ) of the D, G and 2D peak of Raman spectra were analysed. The statistical analysis was conducted according to the procedure described before using the plot of I_G *vs.* Γ_G as filter function (Fig. S4, ESI†) to gain statistically reliable information from single layers of graphene (G_1).[18] The quality of the yielded G_1 is illustrated by plotting the I_D/I_G ratio *vs.* Γ_{2D} as depicted in Fig. 3A. Initially, reference data were collected from films of flakes of ai-GO. Typical Raman spectra of ai-GO (Fig. S6, ESI†) exhibit values of $I_D/I_G \approx 1.0$ and $\Gamma_{2D} \approx 350$ cm^{-1}. Γ_{2D} is extremely broad due to the fact that roughly every second carbon atom of ai-GO is functionalized (sp^3).[9] G_1 (optical image, Fig. S5, ESI†) was analysed by SRM after transferring a film of flakes onto a substrate, followed by reduction with vapours of HI–TFA that have access to the surface from the upper side ($G^{HI/TFA}$). The best quality of G_1 is obtained for this reduction method with an average $I_D/I_G = 3.0 \pm 0.3$ and $\Gamma_{2D} = 62 \pm 8$ cm^{-1} (Fig. 3, red points).

G_1 was also prepared on the reductive subphase (G_{AS}) and transferred on the substrate for analysis. The transferred film of flakes can be characterized by $I_D/I_G = 2.2 \pm 0.2$ and

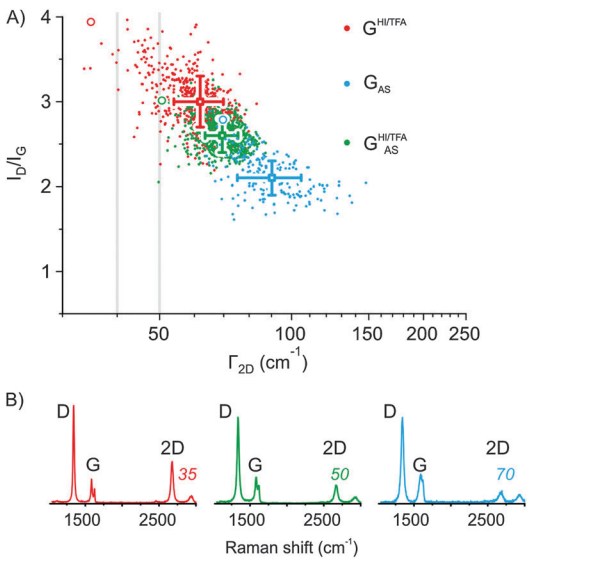

Fig. 3 (A) SRM results illustrated by the plot of I_D/I_G *vs.* Γ_{2D} of G_1 reduced by HI–TFA on a substrate (red, $G^{HI/TFA}$), aqueous solution of AS as the subphase (blue, G_{AS}), combination of both methods (green, $G_{AS}^{HI/TFA}$). (B) Raman spectra of high quality flakes (quality indicated by the coloured circles in red, green and blue in A); italic numbers indicate Γ_{2D}.

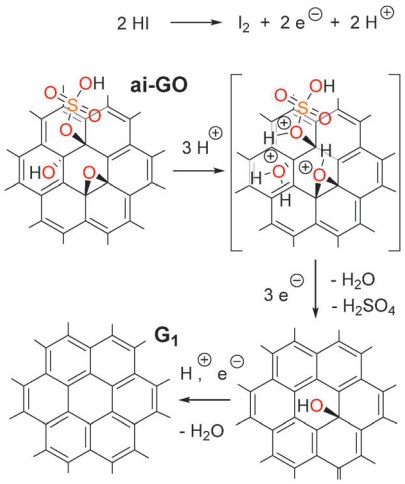

Fig. 4 Reduction of ai-GO by an electron donor, such as iodide and a strong acid, (TFA). Successive protonation an electron transfer steps are proposed to remove oxygen functional groups to form G_1 on a substrate.

Γ_{2D} = 90 ± 15 cm^{-1} (blue). The Γ_{2D} of 90 cm^{-1} is higher and reflects a lower quality of G_1 compared to $G^{HI/TFA}$. However, the reduction was effective, since Γ_{2D} of 90 cm^{-1} is much thinner than Γ_{2D} of 350 cm^{-1} determined for ai-GO. Subsequently, a film of ai-GO, already reduced by the reductive subphase (G_{AS}), was transferred on a substrate and further reduced by vapours of HI–TFA ($G_{AS}^{HI/TFA}$). SRM depicts a narrow quality contribution with I_D/I_G = 2.6 ± 0.2 and Γ_{2D} = 70 ± 6 cm^{-1}. These data illustrate that the quality of G_{AS} can be further improved by HI–TFA treatment. However, the quality remains worse compared to the $G^{HI/TFA}$ (Γ_{2D} = 62, red). This result indicates that the underlying reduction mechanism may be partially hindered by the first reduction step of ai-GO with AS. In accordance to the SRM results (Fig. 3A), Raman spectra of individual flakes of G_1 from the high quality region for each reduction method (Fig. 3B) follow the same trend.

In another experiment ai-GO was floated onto the reductive subphase (AS) and kept floating for 4 days under the reduction conditions. Afterwards, the quality of the flakes of $G_{AS,4d}$ and some few-layer graphene was probed directly on the reductive subphase by SRM without transferring the flakes. From SRM an I_D/I_G = 2.2 ± 0.2 and Γ_{2D} = 77 ± 11 cm^{-1} (Fig. S3, ESI†) was determined without excluding spectra of few-layers of graphene. Therefore, the direct measurement has to be understood as a qualitative trend. Nevertheless, the quality of $G^{HI/TFA}$ (Γ_{2D} = 62) was not attained. Thus, the overall best reduction method is the direct reduction of ai-GO on the substrate with vapours of HI–TFA, even if only the upper side is accessible unhindered by the reducing agent. The whole evaluation process was repeated using HI (1%) as the reductive subphase to form $G_{HI,1\%}$ and it was found that reduction from the subphase is almost as efficient as for $G^{HI/TFA}$ (Fig. S7, Table S1, ESI†).

Thus, a plausible mechanism for the reduction of ai-GO can be derived. A reduction mechanism for GO with HI has been proposed recently that includes the formation of C–I bonds.[7] However, since iodide can be oxidized to iodine an electron transfer from iodide to the residual π-system of ai-GO is plausible (about 50% of C-atoms are sp^2), especially if oxo-functional groups are protonated by a strong acid, as illustrated in Fig. 4. Consequently the transfer of electrons to ai-GO results in an opening of protonated epoxy-groups to hydroxyl-groups (Fig. 4). Protonated organosulfate groups, as well as hydroxyl-groups are cleaved as sulphuric acid and water, respectively, and the positive charge is compensated by electron transfer steps. It can be argued that the reduction of ai-GO proceeds by successive electron transfer steps to the π-system of ai-GO and protonation steps of oxo-functional groups. Since G_1 and ai-GO are 2D-materials it does not matter whether the electrons are transferred from the upper side or the lower side. In contrast to bulky iodide atoms, protons can easily be transferred (proton conductivity) by traces of water between the substrate and ai-GO. Therefore, it can be suggested that hydroxyl-groups (general: oxygen functional groups) can be protonated on both sides, even if ai-GO is placed on a substrate. Since the preparation of G_{AS} is less effective compared to $G_{HI,(1\%)}$ it can be assumed that adsorbed species (between substrate and ai-GO, indicated by AFM, Fig. S1, ESI†) may hamper either the electron transfer or the elimination of functional groups. This reduction mechanism is proposed for intact GO and it should be kept in mind that conventional GO contains structural defects on the several % scale,[5,18] with various functional groups.[27,28]

It was found that one accessible side of ai-GO is sufficient for an efficient reduction to G_1. A general reduction mechanism for the reduction of ai-GO is proposed that involves successive electron transfer steps and protonation steps. If one of these steps is hindered, the full potential reduction will not be possible, which may be the case for less efficient reduction methods.[7] Investigations of reduction kinetics will give further insights into the mechanism and will be addressed in future studies.

The author acknowledges the Deutsche Forschungsgemeinschaft for funding *via* grant EI 938/3-1 and thanks Prof. Dr Andreas Hirsch for his support at FAU Erlangen-Nürnberg. This work is also supported by the Cluster of Excellence 'Engineering of Advanced Materials (EAM)' and SFB 953 funded by the DFG.

Notes and references

1 J. K. Wassei and R. B. Kaner, *Acc. Chem. Res.*, 2013, **46**, 2244–2253.
2 H. Chang and H. Wu, *Adv. Funct. Mater.*, 2013, **23**, 1984–1997.
3 C. Chung, Y. K. Kim, D. Shin, S. R. Ryoo, B. H. Hong and D. H. Min, *Acc. Chem. Res.*, 2013, **46**, 2211–2224.
4 K. S. Novoselov, V. I. Fal'ko, L. Colombo, P. R. Gellert, M. G. Schwab and K. Kim, *Nature*, 2012, **490**, 192–200.
5 S. Eigler and A. Hirsch, *Angew. Chem., Int. Ed.*, 2014, **53**, 7720–7738 (*Angew. Chem.*, 2014, **126**, 7852–7872).
6 F. M. Koehler and W. J. Stark, *Acc. Chem. Res.*, 2013, **46**, 2297–2306.
7 C. K. Chua and M. Pumera, *Chem. Soc. Rev.*, 2014, **43**, 291–312.
8 S. Eigler, S. Grimm, M. Enzelberger-Heim, P. Müller and A. Hirsch, *Chem. Commun.*, 2013, **49**, 7391–7393.

9 S. Eigler, M. Enzelberger-Heim, S. Grimm, P. Hofmann, W. Kroener, A. Geworski, C. Dotzer, M. Rockert, J. Xiao, C. Papp, O. Lytken, H. P. Steinrück, P. Müller and A. Hirsch, *Adv. Mater.*, 2013, **25**, 3583–3587.
10 G. Eda, G. Fanchini and M. Chhowalla, *Nat. Nanotechnol.*, 2008, **3**, 270–274.
11 S. Pei and H.-M. Cheng, *Carbon*, 2012, **50**, 3210–3228.
12 S. Mao, H. Pu and J. Chen, *RSC Adv.*, 2012, **2**, 2643–2662.
13 G. Charpy, *C. R. Hebd. Seances Acad. Sci.*, 1909, **148**, 920–923.
14 B. C. Brodie, *Ann. Chim. Phys.*, 1855, **45**, 351–353.
15 J. William, S. Hummers and R. E. Offeman, *J. Am. Chem. Soc.*, 1958, **80**, 1339.
16 S. Eigler, C. Dotzer, A. Hirsch, M. Enzelberger and P. Müller, *Chem. Mater.*, 2012, **24**, 1276–1282.
17 S. Eigler, S. Grimm, F. Hof and A. Hirsch, *J. Mater. Chem. A*, 2013, **1**, 11559–11562.
18 S. Eigler, F. Hof, M. Enzelberger-Heim, S. Grimm, P. Müller and A. Hirsch, *J. Phys. Chem. C*, 2014, **118**, 7698–7704.
19 M. M. Lucchese, F. Stavale, E. H. M. Ferreira, C. Vilani, M. V. O. Moutinho, R. B. Capaz, C. A. Achete and A. Jorio, *Carbon*, 2010, **48**, 1592–1597.
20 L. G. Cançado, A. Jorio, E. H. M. Ferreira, F. Stavale, C. A. Achete, R. B. Capaz, M. V. O. Moutinho, A. Lombardo, T. S. Kulmala and A. C. Ferrari, *Nano Lett.*, 2011, **11**, 3190–3196.
21 S. Eigler, Y. Hu, Y. Ishii and A. Hirsch, *Nanoscale*, 2013, **5**, 12136–12139.
22 S. Eigler, S. Grimm and A. Hirsch, *Chem. – Eur. J.*, 2014, **20**, 984–989.
23 P. Cui, J. Lee, E. Hwang and H. Lee, *Chem. Commun.*, 2011, **47**, 12370–12372.
24 M. J. Fernández-Merino, L. Guardia, J. I. Paredes, S. Villar-Rodil, P. Solís-Fernández, A. Martínez-Alonso and J. M. D. Tascón, *J. Phys. Chem. C*, 2010, **114**, 6426–6432.
25 S. Eigler, C. Dotzer, F. Hof, W. Bauer and A. Hirsch, *Chem. – Eur. J.*, 2013, **19**, 9490–9496.
26 A. Dimiev, D. V. Kosynkin, L. B. Alemany, P. Chaguine and J. M. Tour, *J. Am. Chem. Soc.*, 2012, **134**, 2815–2822.
27 L. B. Casabianca, M. A. Shaibat, W. W. Cai, S. Park, R. Piner, R. S. Ruoff and Y. Ishii, *J. Am. Chem. Soc.*, 2010, **132**, 5672–5676.
28 W. Gao, L. B. Alemany, L. Ci and P. M. Ajayan, *Nat. Chem.*, 2009, **1**, 403–408.